JOURNAL OF COMPUTATIONAL PHYSICS 59, 56–80 (1985)

A New Approach to Multi-level Non-LTE Radiative Transfer Problems

G. B. SCHARMER*

High Altitude Observatory,
National Center for Atmospheric Research,†
Stockholm Observatory, Saltsjöbaden, Sweden

AND

M. CARLSSON

Uppsala Astronomical Observatory and
Institute of Theoretical Astrophysics,
P.O. Box 1029 Blindern, N-0315 Oslo 3 Norway

Received January 9, 1984; revised June 7, 1984

A new scheme for solving multi-level non-LTE radiative transfer problems is described. In this scheme the radiation field is related to the source function by an approximate radiative transfer operator. This operator is used to set up the linearized nonlocal statistical equilibrium equations for the population numbers with small amounts of computing time. These equations have a characteristic and simple structure which enable a fast solution. The approximate statistical equilibrium equations are combined with the exact rate equations such that the final solution always is exact. The basic methods described can handle velocity fields, partial redistribution, and complex geometries and are ideal for future applications to the numerical solution of radiative hydrodynamics problems with radiation transport in lines and continua. The methods form the basis of a non-LTE program that is more general than the often used code LINEAR-B. Calculations made so far indicate that the new method also is more stable and faster by typically a factor of ten.

1. INTRODUCTION

The transport of radiation in spectral lines plays an important role in determining the energy and momentum balance in the outer layers of stellar atmospheres. One goal of non-LTE (non-local thermodynamic equilibrium) theory is the calculation of the number densities of atoms in various levels and the radiation

* Now at Stockholm Observatory, S-13300 Saltsjöbaden, Sweden.

† The National Center for Atmospheric Research is sponsored by the National Science Foundation.

0021-9991/85 $3.00

fields in the lines, such that these are consistent with one another. The early methods, such as the complete linearization method of Auer and Mihalas [1, 11, 18, 25] were mainly developed for calculating the structure of and radiation coming from stationary atmospheres.

During the last ten years we have witnessed a rapid evolution in the understanding of dynamic phenomena in stellar atmospheres. However, thus far most studies of such problems have included the interactions between radiation and matter in a very primitive way. We know of no such study, for example, which has included the energy transfer in spectral lines in a fully consistent way. The reason for this is that the complexities of these interactions makes numerical solutions extremely expensive. To overcome this barrier, great strides have been made recently to develop new techniques [2, 3] which are very fast, but which sacrifice the high accuracy attainable by present-day standard techniques.

The present paper deals with a new method for the numerical solution of multi-level non-LTE problems. It is ideal for problems involving many frequencies, angles, and depth points. The method is therefore particularly well suited for studies involving velocity fields and it will eventually be included in a radiation hydrodynamics code. The essential idea of the method is to take numerical advantage of certain simplifications which are made possible by the physical nature of emission processes in spectral lines. It is not the purpose of the present article to describe these simplifications in detail; a recent review article by Rybicki [4] contains a thorough account of several aspects of these problems.

Previous work related to the present paper presented a linear iterative technique for solving the equivalent two-level atom non-LTE problem [5], a linearization method for solving the same problem [6, 7] and a linearization method for solving the equivalent two-level problem with partial redistribution [8]. Three years of experience with these methods have convinced us of the usefulness of this approach to non-LTE problems. Future work will concentrate on developing methods for solving many-level problems ($\sim$10–100), non-LTE problems in multi-dimensional geometries and a method for solving multi-level problems with partial redistribution.

The work described in this paper is relevant for studying radiative transfer non-LTE problems. However, the character of the radiative transfer equation as a Boltzman equation suggests that some of the techniques described here may also have applications to other problems.

The outline of this paper is as follows: In Section 2 we formulate the standard non-LTE multi-level problem. In Section 3 we linearize the statistical equilibrium equations (or rate equations) and the radiative transfer equation, closely following Kalkofen [9]. We then show how to precondition [10, 6] the statistical equilibrium equations and the radiative transfer equation in a way which enables the solution of problems with strong numerical cancellation, which arise from "passive" scatterings at large optical depth. In Section 4 we introduce simplifications in the numerical representation of radiative transfer processes, which lead to rapid methods for setting up and solving the statistical equilibrium

equations [5, 7]. In Section 5 we describe some calculations which have been made to test the convergence properties of the present scheme and in Section 6 we briefly outline some generalizations of the present methods.

2. Formulation of the Problem

The solution of a multi-level non-LTE problem involves the simultaneous solution of the statistical equilibrium equations

$$n_i \sum_{j \neq i}^{n_l} P_{ij} - \sum_{j \neq i}^{n_l} n_j P_{ji} = 0, \tag{2.1}$$

the particle conservation equation

$$\sum_{j=1}^{n_l} n_j = n_{\text{tot}}, \tag{2.2}$$

and the radiative transfer equation

$$\mu \frac{dI_{\nu\mu}}{dz} = -\kappa_{\nu\mu} I_{\nu\mu} + j_{\nu\mu}. \tag{2.3}$$

For a discussion of these equations the reader is referred to [1]. In these equations n_i is the number of atoms per unit volume in level i, P_{ij} is the total probability per time unit that an atom in level i will make a transition to level j, $I_{\nu\mu}$ is the specific intensity, $\kappa_{\nu\mu}$ the absorption coefficient, $j_{\nu\mu}$ the emission coefficient, and n_l is the number of atomic energy states considered. The cosine of the angle between the ray and the normal of the atmosphere is equal to μ. The total number of atoms per unit volume is n_{tot}, which is assumed to be a given quantity.

The probabilities P_{ij} can be written as

$$P_{ij} = R_{ij} + C_{ij}, \tag{2.4}$$

where R_{ij} is the contribution from radiative transitions and C_{ij} is the contribution from collisions with other particles. Our main concern here is the radiative transitions, which may be written

$$\begin{aligned} R_{ij} &= A_{ij} + B_{ij}\bar{J}_{ij}, \qquad i > j, \\ &= B_{ij}\bar{J}_{ij}, \qquad i < j \end{aligned} \tag{2.5}$$

for bound–bound transitions. For bound-free transitions essentially the same terms appear (cf. [1, p. 129]). These terms can be included using almost the same procedure as for bound-bound transitions, and they have been included in the general multilevel non-LTE program written by one of the authors [17]. In

Eq. (2.5), A_{ij} is the Einstein spontaneous emission probability and B_{ij} is the coefficient of stimulated emission ($i>j$) and absorption ($i<j$), respectively.

The main source of the numerical difficulties of solving non-LTE problems comes from the quantity $\bar{J}_{ij}$ which may be written

$$\bar{J}_{ij} = \tfrac{1}{2} \int_{-1}^{1} \int_{0}^{\infty} \phi_{\nu\mu} I_{\nu\mu} \, d\nu \, d\mu, \tag{2.6}$$

where $\phi_{\nu\mu}$ is the absorption profile, normalized so that

$$\tfrac{1}{2} \int_{-1}^{1} \int_{0}^{\infty} \phi_{\nu\mu} \, d\nu \, d\mu = 1. \tag{2.7}$$

The quantity $\bar{J}_{ij}$ couples the particle densities n_i to the radiation field, making the problem *nonlocal* and *nonlinear*. The reason for the nonlocality is that the radiation field in principle depends on absorptions and emissions from all points in the gas within the distance over which photons can scatter before they are thermalized. In general this distance is *large*. The reason for the nonlinearity is primarily that the integrated mean intensity $\bar{J}_{ij}$ depends on the population numbers, which makes the statistical equilibrium equations (2.1) nonlinear. Moreover, the intensity $I_{\nu\mu}$ also depends on the population numbers in a nonlinear way, as we shall see shortly. Thus, the calculation of the particle densities n_i, poses a highly coupled, nonlocal and nonlinear problem.

The dependence of the intensity on the population numbers comes from the expressions for the absorption coefficient $\kappa_{\nu\mu}$ and emission coefficient $j_{\nu\mu}$ which in the case of complete redistribution can be written as [1, p. 397]

$$\kappa_{\nu\mu} = \kappa_{\nu c} + \alpha_{ij}(\nu, \mu)(n_i - G_{ij} n_j) \tag{2.8}$$

and

$$j_{\nu\mu} = j_{\nu c} + (A_{ji}/B_{ji}) \, G_{ij} \alpha_{ij}(\nu, \mu) \, n_j \tag{2.9}$$

for $i<j$.

In these equations $\kappa_{\nu c}$ and $j_{\nu c}$ are the background opacities and emissivities, which are here assumed to be known and fixed. It is straightforward to allow them to vary with n_i if necessary. The quantity G_{ij} is equal to the ratio of the statistical weights of the two levels

$$G_{ij} = g_i/g_j = B_{ji}/B_{ij}. \tag{2.10}$$

Equations (2.8) and (2.9) can be used also for bound-free transitions provided the expression (2.10) for G_{ij} is changed and made frequency-dependent [1, p. 397]. For bound-bound transitions the expression for the frequency-dependent cross section is

$$\alpha_{ij}(\nu, \mu) = B_{ij}(h\nu_{ij}/4\pi) \, \phi_{\nu\mu}. \tag{2.11}$$

To close the problem, we finally specify the incoming intensity at the top of the atmosphere and the outgoing intensity at the bottom of the atmosphere. For the purpose of illustrating the basic methods it is sufficient to take $I_\nu(-\mu, \tau_\nu = 0) = 0$ and $I_\nu(\mu, \tau_\nu = \tau_{\max}) = S_{\nu\mu}(\tau_{\max})$, where $S_{\nu\mu}$ is the source function

$$S_{\nu\mu} = j_{\nu\mu}/\kappa_{\nu\mu}. \tag{2.12}$$

For a discussion of a more accurate lower boundary condition, the reader is referred to [1].

3. Linearization and Preconditioning

To solve Eqs. (2.1)–(2.3) we shall employ a multi-dimensional Newton–Raphson method. Such a method was first used and proved to be very successful for non-LTE problems by Auer and Mihalas [11]. This is the only type of scheme which appears sufficiently robust to handle a great variety of problems. However, the present formulation differs from that of Auer and Mihalas in several important respects: First, we use a *Rybicki-type elimination scheme* [12] which is favourable when the number of frequency-angles is large. Second, we linearize the *first-order form of the transfer equation* [9]. This is much simpler than linearizing the second-order form of the transfer equation. Third, we *precondition the statistical equilibrium equations* by eliminating passive scatterings from the equations [6, 10]. This has the advantage of not only increasing the accuracy at large optical depths, but also improving the stability of the solutions, since the dominant nonlinear terms in the rate equations are typically reduced analytically by 4–5 orders of magnitude. Finally, in Section 4 of this paper we show how to combine these methods with the methods of Scharmer [5, 7] for approximating the radiative transfer terms and solving the resulting equations.

3.1. *Linearization of the Rate Equations*

If $n_i^{(n)}$ is a current estimate of n_i which does not satisfy the statistical equilibrium equations exactly, we must write instead of Eq. (2.1),

$$n_i^{(n)} \sum_{j \neq i}^{n_l} P_{ij}^{(n)} - \sum_{j \neq i}^{n_l} n_j^{(n)} P_{ji}^{(n)} = E_i^{(n)}, \tag{3.1}$$

where $E_i^{(n)}$ is an *error term*, corresponding to the imbalance in the net transition rate out of ($E_i^{(n)} > 0$) or into ($E_i^{(n)} < 0$) level i. Since $P_{ij}^{(n)}$ and $E_i^{(n)}$ are determined by $n_i^{(n)}$ we use Eq. (3.1) to calculate $E_i^{(n)}$ after each iteration. From Eq. (2.1) we deduce that the population numbers $n_i^{(n)}$ will converge to the correct values if $E_i^{(n)} \to 0$ for all depths and levels. To obtain the correct solution we now perturb $n_i^{(n)}$ and $P_{ij}^{(n)}$ in such a way that the error terms $E_i^{(n)}$ disappear. Thus if

$$n_i^{(n+1)} = n_i^{(n)} + \delta n_i^{(n)} \tag{3.2}$$

and

$$P_{ij}^{(n+1)} = P_{ij}^{(n)} + \delta P_{ij}^{(n)}, \tag{3.3}$$

we require that the new solution is such that

$$n_i^{(n+1)} \sum_{j=i}^{n_l} P_{ij}^{(n+1)} - \sum_{j=i}^{n_l} n_j^{(n+1)} P_{ji}^{(n+1)} = 0. \tag{3.4}$$

Inserting (3.2) and (3.3) we obtain, by using (3.1) and neglecting all nonlinear terms of the type $\delta n_i^{(n)} \cdot \delta P_{ij}^{(n)}$, a linearized equation in the perturbations $\delta n_i^{(n)}$ and $\delta P_{ij}^{(n)}$,

$$\delta n_i^{(n)} \sum_{j \neq i}^{n_l} P_{ij}^{(n)} + n_i^{(n)} \sum_{j \neq i}^{n_l} \delta P_{ij}^{(n)} - \sum_{j \neq i}^{n_l} \delta n_j^{(n)} P_{ji}^{(n)} - \sum_{j \neq i}^{n_l} n_j^{(n)} \delta P_{ji}^{(n)} = -E_i^{(n)}. \tag{3.5}$$

Using (2.4) and (2.5) we can express $\delta P_{ij}^{(n)}$ in terms of $\delta I_{\nu\mu}^{(n)}$ (since $\delta C_{ij} = 0$ and $\delta \phi_{\nu\mu}$ can be neglected)

$$\delta P_{ij}^{(n)} = B_{ij} \delta \bar{J}_{ij}^{(n)} = B_{ij} \tfrac{1}{2} \int_{-1}^{1} \int_{0}^{\infty} \phi_{\nu\mu} \delta I_{\nu\mu}^{(n)} \, d\nu \, d\mu, \tag{3.6}$$

where $\delta I_{\nu\mu}^{(n)}$ is the perturbation in the intensity which corresponds to the perturbation in the population numbers. To derive a closed set of equations for $\delta n_i^{(n)}$ we must use the linearized transfer equation to express $\delta I_{\nu\mu}^{(n)}$ in terms of $\delta n_i^{(n)}$. This is done in the next section.

3.2. *Linearization of the Transfer Equation*

Let $I_{\nu\mu}^{(n)}$, $\kappa_{\nu\mu}^{(n)}$, and $j_{\nu\mu}^{(n)}$ be current estimates of $I_{\nu\mu}$, $\kappa_{\nu\mu}$ and $j_{\nu\mu}$ such that $I_{\nu\mu}^{(n)}$ is given by

$$\mu \frac{dI_{\nu\mu}^{(n)}}{dz} = -\kappa_{\nu\mu}^{(n)} I_{\nu\mu}^{(n)} + j_{\nu\mu}^{(n)} \tag{3.7}$$

Linearizing (3.7) by perturbing $I_{\nu\mu}$, $\kappa_{\nu\mu}$, and $j_{\nu\mu}$ and neglecting the nonlinear term we obtain [9]

$$\mu \frac{d}{dz} \delta I_{\nu\mu}^{(n)} = -\kappa_{\nu\mu}^{(n)} \delta I_{\nu\mu}^{(n)} - I_{\nu\mu}^{(n)} \delta \kappa_{\nu\mu}^{(n)} + \delta j_{\nu\mu}^{(n)}. \tag{3.8}$$

By defining the monochromatic optical depth $\tau_{\nu\mu}$ in the usual way,

$$d\tau_{\nu\mu}^{(n)} = -\kappa_{\nu\mu}^{(n)} dz/\mu, \tag{3.9}$$

and an *equivalent* source function perturbation $\delta S_{\nu\mu}^{(n)}$ as

$$\delta S_{\nu\mu}^{(n)} = \delta j_{\nu\mu}^{(n)}/\kappa_{\nu\mu}^{(n)} - I_{\nu\mu}^{(n)}\delta\kappa_{\nu\mu}^{(n)}/\kappa_{\nu\mu}^{(n)}, \tag{3.10}$$

we can write Eq. (3.8) in the standard form

$$\frac{d}{d\tau_{\nu\mu}^{(n)}}\delta I_{\nu\mu}^{(n)} = \delta I_{\nu\mu}^{(n)} - \delta S_{\nu\mu}^{(n)}. \tag{3.11}$$

The solution of this equation can be written

$$\delta I_{\nu\mu}^{(n)} = \Lambda_{\nu\mu}^{(n)}[\delta S_{\nu\mu}^{(n)}], \tag{3.12}$$

where $\Lambda_{\nu\mu}^{(n)}$ is a frequency-dependent *linear* integral operator which we define in Section 4.1.

The advantage of linearizing the first-order form of the transfer equation is that this equation contains only one nonlinear term, corresponding to photon absorptions. The nonlinearity of this term is unavoidable, since the number of absorbed photons in a gas is proportional to the number of photons and the number of absorbing atoms. The second-order form of the transfer equation, however, contains nonlinearities which have no obvious physical interpretation, and which makes the linearization procedure much more tedious and probably also less well conditioned.

By linearizing Eqs. (2.8) and (2.9) and combining the results so obtained we may express (3.10) in the form [9]

$$\delta S_{\nu\mu}^{(n)} = c_l^{(n)}\delta n_i^{(n)} + c_u^{(n)}\delta n_j^{(n)}, \tag{3.13}$$

where

$$c_l^{(n)} = -\alpha_{ij}(\nu, \mu)\, I_{\nu\mu}^{(n)}/\kappa_{\nu\mu}^{(n)} \tag{3.14}$$

and

$$c_u^{(n)} = G_{ij}\alpha_{ij}(\nu, \mu)(A_{ji}/B_{ji} + I_{\nu\mu}^{(n)})/\kappa_{\nu\mu}^{(n)}. \tag{3.15}$$

By combining Eqs. (3.12) and (3.13) we see that we have managed to express $\delta I_{\nu\mu}$ as a linear integral operator acting on δn_i and δn_j. Thus we have constructed a complete system of linear equations for the corrections to the population numbers. In the remaining sections we show how to simplify and solve these equations.

3.3. *Preconditioning of the Rate Equations*

Up to this point, our approach has been essentially that of Kalkofen [9]. From now on we incorporate the efficient new tools which have so far been used only to solve linear problems [5–8]. Our first step consists in a preconditioning of the statistical equilibrium equations and of the error terms. This permits the solution of multi-level problems on computers with poor accuracy using single precision

arithmetic. However, the preconditioning is not essential for the methods developed in Section 4.

A very important property of radiation transfer in spectral lines is the enormous variation of the photon mean free path from the core of the line to the wings. A photon emitted close to the center of the line will travel only a very short distance before being reabsorbed, whereas a photon emitted in the far wings may penetrate essentially the whole atmosphere without being reabsorbed. Transfer of radiation in spectral lines therefore occurs most efficiently in the wings of the line whereas the core plays an essentially passive role [10, 13]. It turns out that the passive core components can give rise to numerical problems if the optical depth in the line is very large. To avoid this problem we precondition [10, 6] the equations by introducing a new operator $\delta\Lambda_{\nu\mu}$, defined as the difference between $\Lambda_{\nu\mu}$ and the unity operator, i.e.,

$$\Lambda_{\nu\mu}^{(n)} = 1 + \delta\Lambda_{\nu\mu}^{(n)}. \tag{3.16}$$

Combining (3.5), (3.6), (3.12), (3.13), (3.16) and using the Einstein relations we obtain after some algebra the following set of linear equations for δn_i.

$$\begin{aligned}
\sum_{j=i+1}^{n_l} \Big\{ & B_{ij}(\delta n_i^{(n)} - G_{ij}\delta n_j^{(n)})\,\bar{J}_{\delta ij} + B_{ij}(n_i^{(n)} - G_{ij} n_j^{(n)}) \\
& \cdot \tfrac{1}{2}\int_{-1}^{1}\int_{0}^{\infty} \phi_{\nu\mu}\delta\Lambda_{\nu\mu}^{(n)}[c_l^{(n)}\delta n_i^{(n)} + c_u^{(n)}\delta n_j^{(n)}]\,d\nu\,d\mu \\
& - A_{ji}\delta_{ij}^{(n)}\delta n_j^{(n)} + \delta n_i^{(n)} C_{ij} - \delta n_j^{(n)} C_{ji} \Big\} \\
& + \sum_{j=1}^{i-1} \{\text{similar terms}\} = -E_i^{(n)}.
\end{aligned} \tag{3.17}$$

In this equation $\delta_{ij}^{(n)}$ and $\bar{J}_{\delta ij}^{(n)}$ are defined as

$$\delta_{ij}^{(n)} = \frac{1}{2}\int_{-1}^{1}\int_{0}^{\infty} \frac{\kappa_{\nu c}}{\kappa_{\nu\mu}^{(n)}}\,\phi_{\nu\mu}\,d\nu\,d\mu \tag{3.18}$$

and

$$\bar{J}_{\delta ij} = \frac{1}{2}\int_{-1}^{1}\int_{0}^{\infty} \frac{\kappa_{\nu c}}{\kappa_{\nu\mu}^{(n)}}\,I_{\nu\mu}^{(n)}\,\phi_{\nu\mu}\,d\nu\,d\mu. \tag{3.19}$$

Although Eq. (3.17) appears slightly more complicated than Eq. (3.5) it is much more advantageous from a computational point of view, since the dominant terms have been reduced by approximately a factor δ. Since δ is on the order of 10^{-5} or less for strong lines we can see that preconditioning has removed the main reason for the numerical cancellation at large optical depths. Note also that of the terms which were orginally nonlinear, only two small contributions now remain. The first

comes from interactions with the continuum. The second and more important contribution comes from the nonlocal term, i.e., from the term containing the $\delta\Lambda_{\nu\mu}$-operator. Preconditioning therefore emphasizes that the nonlinearity is primarily connected to the fact that non-LTE problems are nonlocal. Since preconditioning reduces the nonlinear terms by many orders of magnitude, it seems reasonable to suppose that it may also be important in preventing numerical instabilities from developing.

Finally, we point out that the often-made assumption of "detailed balance in the lines" [14] is somewhat questionable. What actually happens at great optical depth is that $I_{\nu\mu} \to S_{\nu\mu}$ which is equivalent to saying that the nonlocal term containing $\delta\Lambda_{\nu\mu}$ disappears. But, as is evident from (3.17), we may still have interactions with the overlapping continuum which destroys the detailed balance in the lines. We therefore suggest that rather than assuming detailed balance in the lines, it is better to assume that $\delta\Lambda_{\nu\mu} \to 0$. The system of equations thus obtained will still be nonlinear but local, which makes the numerical solution simple.

3.4. *Preconditioning of the Error Terms*

To obtain high accuracy in the converged solution we must calculate the error terms accurately. To do this we must also precondition the calculation of the error terms $E_i^{(n)}$ as defined by (3.1). By adding and subtracting $S_{\nu\mu}$ from $I_{\nu\mu}$ we obtain

$$\begin{aligned} E_i^{(n)} = \sum_{j=i+1}^{n_l} & \{B_{ij}(n_i^{(n)} - G_{ij} n_j^{(n)})(\bar{J}_{ij}^{(n)} - \bar{S}_{\nu\mu}^{(n)}) \\ & - A_{ji}\delta_{ij}^{(n)} n_j^{(n)} + B_{ij}(n_i^{(n)} - G_{ij} n_j^{(n)})\, \delta_{ij}^{(n)} \bar{S}_{c\nu} \\ & + n_i^{(n)} C_{ij} - n_j^{(n)} C_{ji}\} + \sum_{j=1}^{i-1} \{\text{similar terms}\}, \end{aligned} \tag{3.20}$$

where

$$\bar{J}_{ij}^{(n)} - \bar{S}_{\nu\mu}^{(n)} = \tfrac{1}{2} \int_{-1}^{1} \int_{0}^{\infty} \phi_{\nu\mu} (I_{\nu\mu}^{(n)} - S_{\nu\mu}^{(n)})\, d\nu\, d\mu \tag{3.21}$$

and

$$\bar{S}_{c\nu} = \frac{1}{2} \int_{-1}^{1} \int_{0}^{\infty} \frac{\kappa_{\nu c}}{\kappa_{\nu\mu}^{(n)}} \cdot \frac{j_{\nu c}}{\kappa_{\nu c}} \phi_{\nu\mu}\, d\nu\, d\mu / \delta_{ij}^{(n)}. \tag{3.22}$$

The whole purpose of writing Eq. (3.20) in this form is that $\bar{J}_{ij}^{(n)} - \bar{S}_{\nu\mu}^{(n)}$ can be calculated very accurately at large optical depths using the standard Feautrier technique [6] to calculate $P_{\nu\mu} - S_{\nu\mu}$ from

$$P_{\nu\mu} - S_{\nu\mu} = \frac{d^2 P_{\nu\mu}}{d\tau_{\nu\mu}^2}, \tag{3.23}$$

where $P_{\nu\mu}$ is the average of the incoming and outgoing intensities.

We emphasize that the accuracy in the final solution depends only on the accuracy with which $E_i^{(n)}$ is calculated, and is independent of the approximations that are made to generate the approximate equation for δn_i. A coarse frequency-angle grid would lead to poor accuracy in the final solution, but does not significantly affect convergence since the same *type* of errors is made in the representation of the matrix and in the calculation of error terms.

4. Method of Solution

So far we have been concerned mainly with setting up the multi-level non-LTE problem in such a way that we eliminate much of the nonlinearity from the problem. This procedure also gives high accuracy at large optical depths. In this section we concentrate on developing an efficient scheme for iterating the solution of Eqs. (3.17) towards convergence. As pointed out in Section 3.4 we are free to choose whatever approximations we like in the calculation of the approximate corrections δn_i. However, to obtain rapid convergence it is important to choose approximations which are qualitatively correct in essential respects. If this is not done, the solution will diverge or converge very slowly.

For non-LTE problems with comparatively few levels and depth points, the time required to *set up* the matrix corresponding to the integral equations for δn_i dominates the total computing time. For problems with more depth points and levels, the time required to *solve* the matrix equation dominates. The essential idea of the present method for solving non-LTE problems is to introduce approximations which simplifies both the numerical representation and the solution of the matrix equation [5, 7]. Since the nonlocalness introduced by the radiation field is the major reason for the numerical difficulties of solving non-LTE problems we have concentrated on simplifying the numerical representation of radiation transport mechanisms. The present *numerical method* is therefore intimately connected to the *physics of the problem.*

4.1. *Approximating the Linearized Rate Equations*

The solution of Eq. (2.3) can be written

$$I^+_{\nu\mu}(\tau_{\nu\mu}) = \Lambda_{\nu\mu}[S_{\nu\mu}] \equiv e^{\tau_{\nu\mu}} \int_{\tau_{\nu\mu}}^{\infty} S_{\nu\mu}(\tau'_{\nu\mu})\, e^{-\tau'_{\nu\mu}}\, d\tau'_{\nu\mu} \tag{4.1}$$

for an outgoing ($\mu > 0$) ray. In this equation $S_{\nu\mu}$ is the source function as defined by (2.12). If $S_{\nu\mu}$ varies much more slowly than $\exp(-\tau_{\nu\mu})$, then most of the contribution to $I_{\nu\mu}$ comes from a fairly narrow range in $\tau_{\nu\mu}$. By assuming that $S_{\nu\mu}$ is linear in $\tau_{\nu\mu}$ we can estimte (4.1) by a one-point numerical quadrature formula of the type [5, 7]

$$I^+_{\nu\mu}(\tau_{\nu\mu}) \approx \Lambda^+_{\nu\mu}[S_{\nu\mu}] \equiv \omega^+ S_{\nu\mu}(\tau^+_{\nu\mu}). \tag{4.2}$$

For a semi-infinite medium the quadrature weight ω^+ is equal to one and the quadrature point $\tau^+_{\nu\mu}$ is given by

$$\tau^+_{\nu\mu} = \tau_{\nu\mu} + 1. \tag{4.3}$$

For a finite medium the expressions for ω^+ and $\tau^+_{\nu\mu}$ are different [7].

For an incoming ray ($\mu < 0$) we obtain similar quadrature formulae, but the expressions for the weight and the quadrature point are now somewhat more complicated

$$\omega^- = 1 - e^{-\tau_{\nu\mu}}, \qquad \tau^-_{\nu\mu} = \tau_{\nu\mu}/\omega^- - 1. \tag{4.4}$$

In practical applications we set $\omega^- = 0$ when $\tau_{\nu\mu} < 0.1$ and use a diffusion approximation for $\tau_{\nu\mu} > 10$. Therefore, very few exponentials have to be calculated. The computing of exponentials is always an insignificant part of the total computing time.

The advantage of using the one-point quadrature approximate relations between $I_{\nu\mu}$ and $S_{\nu\mu}$ is that they require only $O(n_\tau)$ operations as compared to the $O(n_\tau^2)$ operations required by other methods. Since n_τ may typically be in the range 100–200 for problems involving large amplitude velocity fields the gain in computing time may be considerable. In spite of the simplicity, the quadrature formulae defined by (4.2)–(4.4) give errors in the population numbers which are only on the order of 20%. Note, however, that these approximate statistical equilibrium equations are combined with the *exact* rate equations such that the *final* solution is exact.

Another important advantage of these approximations is that the quadrature point for the incoming rays, $\tau^-_{\nu\mu}$, goes towards $\tau_{\nu\mu}/2$ at small optical depths. Physically, this happens because the radiation coming from very small optical depths tends to be weak, since the emission coefficient scales roughly as the absorption coefficient. When solving non-LTE problems, we typically use five or six depth points per decade in optical depth. On such a depth scale the point $\tau_{\nu\mu}/2$ is less than two depth points away from $\tau_{\nu\mu}$ and thus the incoming radiation field is nearly local. Therefore, the numerical implementation of (4.4) results in a matrix which has a strongly upper triangular structure, as regards the spatial interactions. This structure permits a very fast solution of the matrix equation.

To represent the statistical equilibrium equations, Eq. (3.17), numerically we replace the "exact" radiation transport operator $\delta\Lambda^{(n)}_{\nu\mu}$ by the approximations implied by (4.2) and (4.4). The depth points $\tau^+_{\nu\mu}$ and $\tau^-_{\nu\mu}$ will usually be located in between two grid points. To represent $S_{\nu\mu}(\tau^+_{\nu\mu})$ or $S_{\nu\mu}(\tau^-_{\nu\mu})$, we simply assume that $S_{\nu\mu}$ varies linearly between the two grid points closest to the quadrature point. These two grid points can be searched for rapidly by noting that $\tau^+_{\nu\mu}$ and $\tau^-_{\nu\mu}$ are monotone increasing functions of $\tau_{\nu\mu}$ and that $\tau_{\nu\mu}$ increases monotonically with depth [5]. To represent the double integrals we use Gaussian quadrature for the angle integration and the trapezoidal rule for the frequency integration (see also [7]). The discretization of Eq. (3.17) is in fact very simple.

The linear interpolation formula used to represent $S_{\nu\mu}(\tau^+_{\nu\mu})$ gives serious numerical inaccuracies at large optical depths [6]. To avoid this problem it is usually sufficient to set $\delta\Lambda^+_{\nu\mu}=0$ when $\tau_{\nu\mu}\geqslant 100$. For certain problems with continuum scattering [4, 10] it is much better to include a diffusion term for large and moderately large optical depths

$$\delta\Lambda^\dagger_{\nu\mu}[S_\nu]=\frac{dS_{\nu\mu}}{d\tau_{\nu\mu}}+\frac{d^2S_{\nu\mu}}{d\tau^2_{\nu\mu}}; \qquad \Delta\tau_{\nu\mu}\geqslant 5, \tag{4.5}$$

where $\Delta\tau_{\nu\mu}$ is the difference in optical depth between two neighbouring grid points.

The computing time required to set up the approximate rate equations using the method of this paper scales as

$$t=c_1\cdot n_{\mathrm{tr}}\cdot n_\tau\cdot n_\mu\cdot n_\nu. \tag{4.6}$$

where n_{tr} is the number of radiative transitions, n_τ the number of depth points and $n_\mu n_\nu$ is the number of frequency-angles. The time required for setting up this matrix is always less than the time required to solve a similar LTE problem. This is a reasonable computational effort.

4.2. *Approximations Made at Small Optical Depths*

The most distant interactions occur in the wings of spectral lines where the optical depth is small. As emphasized in Section 3.3 nonlocality is the most important source of nonlinearity. The treatment of radiation transport in the thin wings of the lines is therefore of considerable importance for the numerical stability of the solution.

The calculations made so far indicate that the best approach to eliminating numerical instabilities is simply to set

$$\Lambda^\dagger_{\nu\mu}=0$$

at small optical depths, $\tau_{\nu\mu}<0.1$. This implies that the influence on the population numbers of the optically thin components of the radiation field is corrected for by lambda iteration, i.e., these particular components of the radiation field are lagged one iteration. In principle this could lead to somewhat slower convergence. Our test calculations indicate that this is not the case and that other important advantages are gained.

In the optically thin limit the population numbers are governed by the radiation field whereas the influence of the population numbers on the radiation field is fairly weak and lambda iteration does not produce numerical instabilities. More important, however, is that lambda iteration guarantees that the radiation field used to calculate the population numbers is physically meaningful whereas in a nonlocal linearization scheme we have no guarentee that the specific intensity *implied* in the linearization will even be positive! In this respect lambda iteration is much safer than linearization which can produce physical inconsistencies, such as the

occurrence of negative population numbers which usually lead to numerical instabilities.

These numerical problems with the nonlocal radiation field were initially discovered when we attempted to solve the five-level Calcium problem with the VAL3-C model [15] using a depth grid which extended up to very high chromospheric temperatures. In the first iterations we found negative population numbers in the uppermost layers where the optical depth at line center of the Ca–K line was on the order of 10^{-5}. This was not expected on physical grounds, since in these layers the population numbers are almost entirely determined by the radiation field coming from below, and the non-LTE problem should be linear and trivial. The occurrence of negative population numbers came from the *nonlocal* matrix elements which coupled the local changes in the population numbers to the depth where the optical depth in the K-line was of order unity. Here the neglect of the *nonlinear* terms gave sufficiently large errors to produce unphysical answers. The whole problem disappeared completely when $\Lambda^{\dagger}_{\nu\mu}$ was set to zero for $\tau_{\nu\mu} < 0.1$. These results indicate that these nonlinearities are caused by the fact that the nonlocal radiation field is bi-directional.

Setting $\Lambda^{\dagger}_{\nu\mu} = 0$ also eliminates the most nonlocal matrix elements which creates a more or less pronounced band structure in the matrix equations. This property should be taken advantage of when solving these equations.

4.3. *Solution of the Matrix Equation*

The grand matrix of Eq. (3.17), which has the size $(n_\tau n_l) \times (n_\tau n_l)$, is assembled transition by transition. Looping over all frequency-angles we add up all the $\delta\Lambda_{\nu\mu}$-operators with their corresponding weights into the linearized rate matrix. In the same frequency-angle loop the intensities $I_{\nu\mu}$, corresponding to the population numbers of the previous iteration, are calculated. These intensities are needed for the calculation of the $\delta\Lambda_{\nu\mu}$ operators, the E_i terms and the $\bar{J}_{\delta ij}$ terms. Since no frequency or angle-dependent quantities need to be stored, it is only the rate matrix itself that needs core memory. Furthermore, we renormalize the matrix so that the solution vector corresponds to the *relative* change of the population numbers

$$\delta b_i^{(n)} = \delta n_i^{(n)} / n_i^{(n)}, \tag{4.7}$$

where $n_i^{(n)}$ are the population numbers of the previous iteration. This has the effect of decreasing the variation of $c_u^{(n)}$ and $c_l^{(n)}$ with depth which decreases the errors introduced by representing these functions with linear interpolation formulae.

The equations are stored in the following order: For each depth point we first store the linearized particle conservation equation (2.2), which replaces the rate equation for level 1. Then on each of the following $n_l - 1$ rows, we store the remaining rate equations for that depth. The next row contains the particle conservation equation for the next depth, and so on. Figure 1 shows the ordering of a matrix with six levels. The matrix consists of blocks, each containing $n_l \times n_l$ elements. The off-diagonal blocks contain the interactions with other depths. These

INFLUENCE ON			INFLUENCE FROM depth 1						depth 2						depth 3					
			level 1	level 2	level 3	level 4	level 5	level 6	level 1	level 2	level 3	level 4	level 5	level 6	level 1	level 2	level 3	level 4	level 5	level 6
depth 1		level 1	X	X	X	X	X	X	0	0	0	0	0	0	0	0	0	0	0	0
		level 2	X	X	X	X	X	X	0	X	0	X	X	X	0	X	0	X	X	X
		level 3	X	X	X	X	X	X	0	0	X	0	X	X	0	0	X	0	X	X
		level 4	X	X	X	X	X	X	X	X	0	X	0	X	X	X	0	X	0	X
		level 5	X	X	X	X	X	X	X	X	X	0	X	X	X	X	X	0	X	X
		level 6	X	X	X	X	X	X	X	X	X	X	X	X	X	X	X	X	X	X
depth 2		level 1	0	0	0	0	0	0	X	X	X	X	X	X	0	0	0	0	0	0
		level 2	0	X	0	X	X	X	X	X	X	X	X	X	0	X	0	X	X	X
		level 3	0	0	X	0	X	X	X	X	X	X	X	X	0	0	X	0	X	X
		level 4	X	X	0	X	0	X	X	X	X	X	X	X	X	X	0	X	0	X
		level 5	X	X	X	0	X	X	X	X	X	X	X	X	X	X	X	0	X	X
		level 6	X	X	X	X	X	X	X	X	X	X	X	X	X	X	X	X	X	X

FIG. 1. Ordering of equations and unknowns for an atomic model with 6 levels. Row number one represents the linearized equation of particle conservation for depth point number one in the atmosphere. The next five rows represent the linearized local and nonlocal equations of statistical equilibrium of that atomic level at the same depth point. It is assumed that transitions $1 \rightarrow 2$, $1 \rightarrow 3$, $2 \rightarrow 3$, $3 \rightarrow 4$, and $4 \rightarrow 5$ are radiatively forbidden. The equations for the other depth points follow.

interactions come from the nonlocal components of the radiation field. It is this radiation field that destroys the diagonal structure of the grand matrix, thus being the source of the numerical expense of solving the matrix equation.

As mentioned earlier, this radiation is almost local, which implies that *most blocks far from the main diagonal contain only zeroes.* In fact, as we go sufficiently high up in the atmosphere, all lines become optically thin and *all* off-diagonal blocks contain zeroes. On the other hand, as we go sufficiently deep down into the atmosphere all transitions become optically thick. In this limit we set $\delta\Lambda^{\dagger}_{\nu\mu} = 0$ or make the diffusion approximation. At large depths, the matrix therefore contains zero or one block to the left of the main diagonal.

From the discussion above it should be evident that the structure of the approximate rate-matrix is completely determined by our treatment of nonlocal radiative interactions occurring in the spectral lines. The approximate methods described in this and the previous sections simplify the numerical representation of these interactions in a way which allows an efficient solution method.

We eliminate all nonzero elements to the left of the diagonal by ordinary Gaussian elimination. A test whether they are nonzero saves on the order of $n_l n_\tau$ multiplications per zero element. The computing time required to solve the matrix equation roughly scales as

$$t = c_2 n_\tau^2 n_l^3 + c_3 n_l^2 n_\tau^2. \tag{4.8}$$

This scaling assumes that we are using a given number of depth point per decade in optical depth. The first term corresponds to the LU factorization and the second to

the "backsubstitution" process. This compares favorably with the Rybicki elimination scheme [12] for which the computing time is proportional to $n_\tau^3 n_l^3$.

4.4. *The Iteration Algorithm*

To summarize the most important steps of the present method, we give here the iteration algorithm used for solving multi-level, non-LTE problems:

(I) Initialize the population numbers by a first guess of the radiation field. Starting approximations like $I_{\nu\mu} = B_\nu$, where B_ν is the Planck function, or $I_{\nu\mu} = 0$ [16] usually are sufficient for final convergence (although somewhat more realistic starting approximations may sometimes be needed, see below, Section 5.2).

(II) Set up the linearized, preconditioned rate equations (3.17) for $\delta n_i/n_i$ using the approximate $\delta\Lambda^+_{\nu\mu}$-operator. At the same time calculate the error terms E_i and the $\bar{J}_{\delta ij}$ terms.

(III) Solve the resulting matrix equation by Gauss elimination of nonzero matrix elements. Update the population numbers $n_i^{(n+1)} = n_i^{(n)} + \delta n_i^{(n)}$.

(IV) Test for convergence. Return to (II) unless max $|\delta n_i^{(n)}/n_i^{(n)}|$ is sufficiently small.

Usually the matrix equation does not change much after two or three iterations. It is therefore sufficient only to set up this matrix and LU-factorize it two or three times; during the last iterations we only need to calculate the error terms and perform the back substitution with the previous $\delta\Lambda$ operator.

5. Numerical Results

The methods developed in the previous sections have been implemented in a general FORTRAN-77 program [17]. This program solves multi-level problems with lines, overlapping continua, and photoionization continua and is more general than the code LINEAR, described by Auer *et al.* [18].

Some tests were made using parametrized atomic models and atmospheres. However, we discovered that realistic atomic and atmospheric models posed much more difficult problems. Two such calculations will be described here: a five level + continuum calcium problem and a three level + continuum hydrogen problem. The model atmosphere used in both cases was the VAL3-C solar atmosphere model [15]. The electron densities were taken from the VAL3-C model and kept fixed.

5.1. *Calcium II*

A five-level + continuum atomic model was used with crosssections for collisional excitation and ionization from [19]. The photoionization rates were calculated from given radiation temperatures. Five radiative transitions were included: the H and K lines and the IR-triplet. Voigt profiles were used for all five lines with microturbulence contributing to the Doppler width and with radiative,

van der Waals and Stark broadening considered. Forty-five depth points, 3 angle points, and 30 frequency points per line were used.

Three different initializations were tried: $I_{\nu\mu} = B_\nu$, $I_{\nu\mu} = 0$, and two successive lambda-iterations from $I_{\nu\mu} = B_\nu$. All three lead to good convergence. With $I_{\nu\mu} = 0$ as initialization, the initial population numbers departed by as much as a factor 10^3 from the converged solution. In spite of this very large initial error, the population numbers converged rapidly, as is shown in Fig. 2.

This problem was solved with the same frequency, angle, and depth points using the code LINEAR-B [18]. The maximum relative difference between the two solutions was 1.3% in the population numbers and 2.5 % in the calculated line profiles. The differences are attributed to differences in background opacity routines and the coarse depth grid which gives different types of errors in the two programs. Both programs required five iterations to give a maximum relative error of less than 0.1% in the population numbers. The CPU-time used on a CYBER 170/835 computer was 300 sec for LINEAR-B and 30 sec for the present program (in no case including initialization and printouts).

5.2. *Hydrogen*

A three level + continuum atomic model was used with cross sections for collisional excitation from [20, 21] and for collisional ionization from [22]. The Lyman continuum was solved in detail while the Balmer and Pachen continua were represented with radiation temperatures. Three lines were included: Lyman-α, Lyman-β, and H-α, all with Voigt profiles. The Voigt-profiles for Ly-α and Ly-β

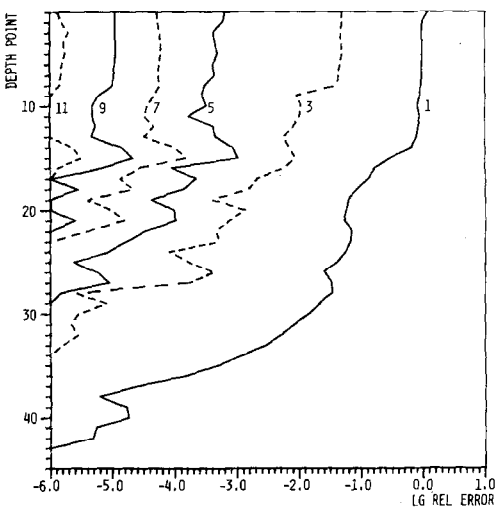

FIG. 2. Log(relative error) after iteration 1–11 for a calculation with a five level + continuum calcium atom and the VAL3-C solar model atmosphere. The relative error is defined as $\max|(n_i^{(n)} - n_i^{(\infty)})/n_i^{(\infty)}|$.

were truncated at 6 Doppler-widths to mimic the effects of partial redistribution on the population numbers [23]. Sixty depth points, 3 angle points, 20 frequency points per line, and 10 frequency points in the Lyman continuum were used.

Three different initializations were tried. $I_{\nu\mu}=0$ and $I_{\nu\mu}=B_\nu$ led to numerical instabilities while initializing by two successive lambda iterations from $I_{\nu\mu}=B_\nu$ leads to a smooth convergence, as is shown in Fig. 3. A maximum relative error of less than 0.1% in the population numbers required 8 iterations and 35 CPU sec on a CYBER 170/835 computer (not including initialization and printouts).

We also tried to solve this problem with the same frequency, angle, and depth points using the code LINEAR-B. It was, however, not possible to get convergence. A much more complicated starting solution was needed for this code—the standard procedure is to start with a simpler atomic model with only the Lyman continuum treated in detail and iterate to convergence. Next, this solution is used as a starting solution for additional iterations which also include the *Ly-α* line. The third step, finally, is to treat the full three level + continuum model atom with the Lyman continuum and the *Ly-α*, *Ly-β*, and $H-\alpha$ lines included [16].

The fact that such a complicated procedure was not needed with the present program indicates good numerical stability. Also coarse depth grids led to a converged solution. Another indication is the total absence of artificial more or less adhoc fix-ups in attempts to prevent such things as negative population numbers.

The whole iteration process for hydrogen is, however, more sensitive than for calcium to the depth scale used. A sufficiently dense grid is necessary in the narrow zone where the degree of ionization changes rapidly. The present program contains

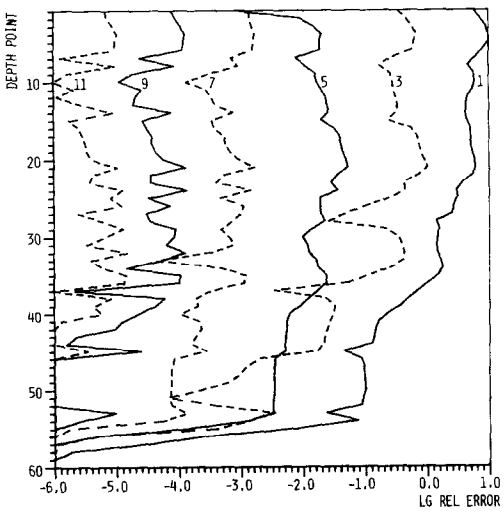

FIG. 3. Log(relative error) after iteration 1–11 for a calculation with a three-level + continuum hydrogen atom and the VAL3-C solar model atmosphere.

routines for establishing optimized depth scales; the reader is referred to [17] for details and a discussion of this aspect.

5.3. *Structure of the Matrices*

In Fig. 4 the grand matrix of the hydrogen calculation is shown in a coded form. Each symbol represents one matrix element in the $(n_\tau n_l \times n_\tau n_l)$ matrix. Increased darkness of the symbol denotes increased size of the element compared with the sum of all elements of that row; white represents elements identically equal to zero. A diagonal composed of dark (4×4) small matrices can be discerned. These small matrices represent the *local* influence. The first row of the small matrices represents the equation of particle conservation while the other rows represent the equations of statistical equilibrium. All the off-diagonal blocks contain the *non local* influence. At a certain depth the blocks to the *left* of the diagonal represent the influence on

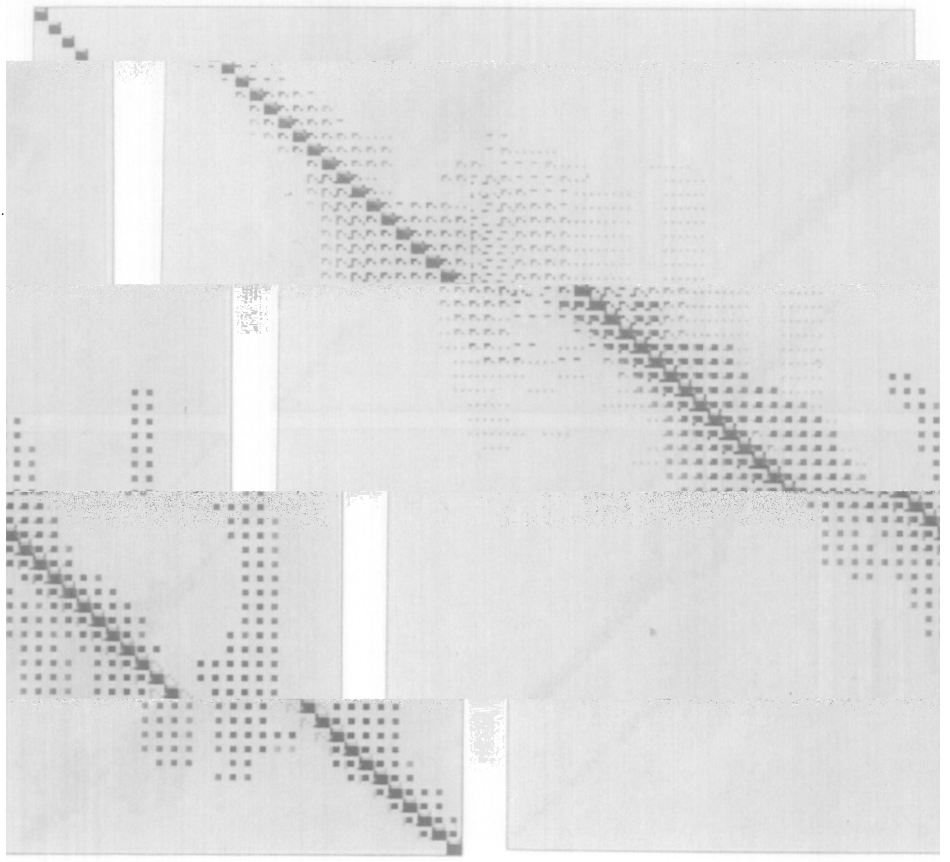

FIG. 4. The grand matrix of a hydrogen calculation. Darker symbols denote larger matrix elements.

the population numbers at that depth from depth points *higher up* in the atmosphere. This influence is carried by the *incoming* radiation. The off-diagonal blocks to the *right* represent influence from the *lower* layers carried by the *outgoing* radiation field.

Several features are readily apparent: the absence of blocks far off the diagonal and a band structure. The bands are due to the discretization in angle and frequency and the fact that the optical depth in the H-α line is quite constant from depth point 30–50. Such zones with very small opacity in some frequency-angles also result in widenings of the diagonal band: the photons can travel further before they interact.

The absence of elements far from the diagonal to the *left* is due to the properties of the approximate radiative transfer operator $\Lambda^{\dagger}$ (see Section 4.1).

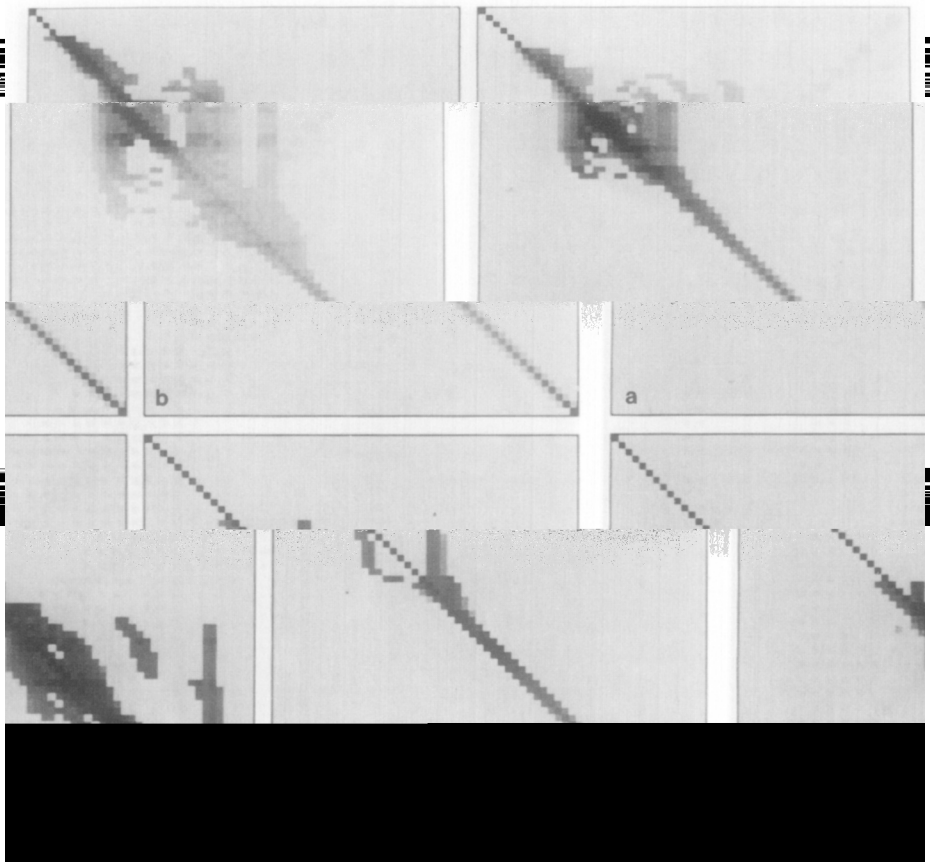

FIG. 5. The structure of the nonlocal interactions, shown transition by transition. Transitions: (a) *Ly*-α, (b) *Ly*-β, (c) *H*-α, (d) Lyman continuum.

The absence of elements far from the diagonal to the *right* is due to the fact that the outgoing radiation field is lambda iterated when $\tau_{\nu\mu} > 0.1$.

Another way of displaying the matrix is to separate the influence on the matrix from the different lines and continua. Such a representation is shown in Fig. 5. Each symbol denotes the contribution from one transition to one *block* of the grand matrix. When $\tau_{\nu\mu} < 0.1$ for all frequency-angles of the transition we have a strictly diagonal structure because of the lambda iteration of those optically thin components of the radiation field. When the transition is treated in the diffusion approximation a tridiagonal structure results.

The wide structure of the matrix for the Lyman continuum is caused by the dense

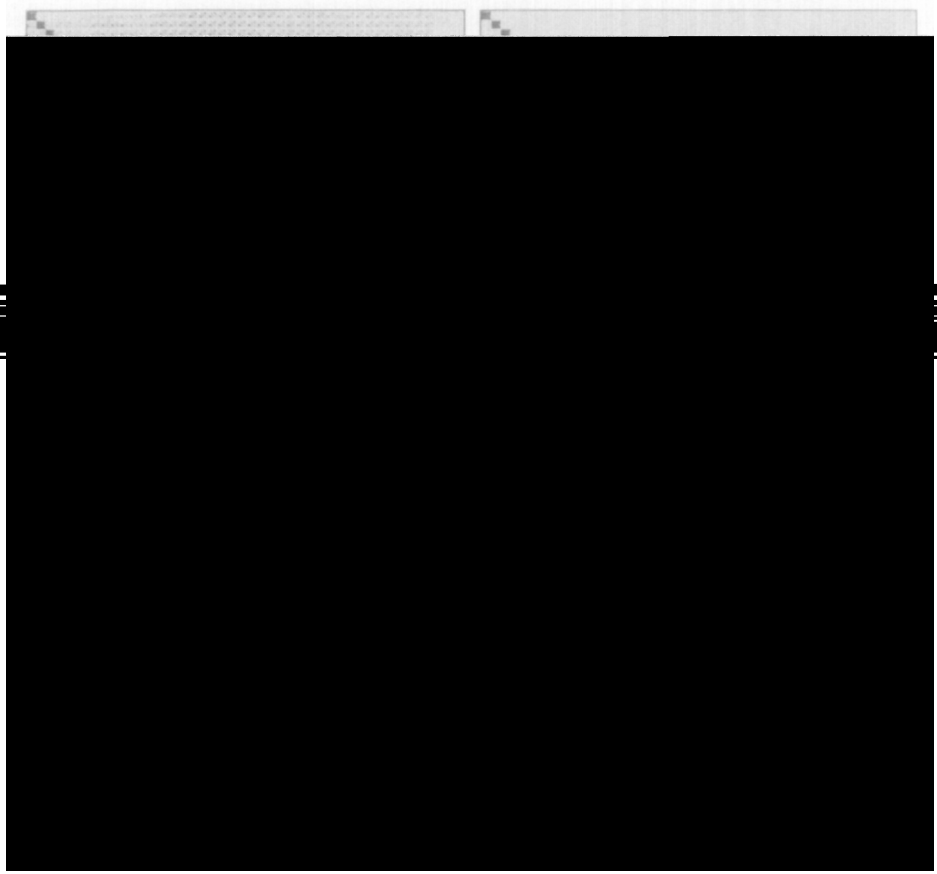

FIG. 6. The grand matrix of four different calcium calculations: (a) zero microturbulence, no macroscopic velocity field, no lambda iteration; (b) zero microturbulence, no macroscopic velocity field, lambda iteration for $\tau_{\nu\mu} < 0.1$; (c) with microturbulence from VAL3-C, no macroscopic velocity field, with lambda iteration for $\tau_{\nu\mu} < 0.1$; (d) zero microturbulence, with macroscopic velocity field, with lambda iteration for $\tau_{\nu\mu} < 0.1$.

depth-grid in the zone where hydrogen is ionized, and corresponding widenings of the diagonal band structure can be seen for *Ly-α* and *Ly-β* and for *H-α* in the lower layers.

In Fig. 6 we have four matrices from calcium five-level + continuum problems. Figure 6a shows the appearance of a calculation with constant microturbulence and no lambda iteration of the thin components of the radiation field. Figure 6b shows the same problem but with the thin components lambda iterated. Those two matrices demonstrate clearly that the absence of elements to the far right is due to the lambda iteration while the absence of elements to the far left is due to the approximate radiative transfer operator $\Lambda^{\dagger}$ itself.

Figure 6c shows the matrix of a calcium calculation with a microturbulence variable with depth. The effect of this is that the lines are broadened more in the upper parts of the atmosphere. At some frequencies in the wings of the line deep down, we have almost no opacity and we can therefore see the broadened line core far above. The photons travel further before they interact and the result is more off-diagonal elements. This increased nonlocality is somewhat similar to the effect of a macroscopic velocity field; see Fig. 6d. There a calculation with zero microturbulence but with a systematic velocity field is shown. The macroscopic velocity field chosen is similar to those obtained from hydrodynamic calculations of free oscillations in the solar chromosphere [26].

The simple structure of the matrix with a more or less pronounced diagonal structure is taken advantage of when solving the system of equations. This results in considerable savings of computing time.

5.4. *CPU-Usage, Memory, and Accuracy Requirements*

The calculations were carried out with a CYBER 170/835 computer with a word length of 60 bits. The CPU-time used by the different parts of the program can be found in Table I. It is interesting to note that only 50% of the total time is spent on tasks directly related to the solution of the non-LTE problem.

The memory requirement is totally dominated by the storage of the grand matrix which needs $n_\tau^2 \times n_l^2$ words of memory. In the two problems discussed here, that matrix took over 80% of the memory used.

One mega-word (M word) of memory is today quite common (would allow 20 level problems to be solved with 50 depth points) and 256 M words will soon be available.

The problems discussed in Sections 5.1 and 5.2 were also solved on a VAX-11/750 computer using single precision arithmetics (word length of 32 bits). The population numbers agreed to typically within 10^{-6} of those obtained from the calculations with the CYBER 170/835 (word length of 60 bits) except in the uppermost seven depth points for hydrogen where the difference was up to 10^{-4}. All calculated fluxes agreed to within 5×10^{-6}.

The fact that the accuracy obtained in the VAX-calculations was almost at the level of the machine accuracy is a result of the preconditioning of the equations.

TABLE I

CPU-Usage of Different Routines (Cyber 170/835)

Routine	Ca (%)	H (%)
Background opacities	5	10
Voigt profiles	1	1
Initializations	8	4
Disc I/O	12	15
Printouts	20	17
Normalizing matrices	3	6
Error calculation	20	14
Set-up of matrices	13	13
Solving matrix equations	18	21
Total (sec)	57	65

5.5. *Performance on a* CRAY-1

The program has been run extensively on the CRAY-1 at SAAB in Linköping. We report here on our experience with respect to the vectorization of certain central parts of the program.

Essentially the program consists of three parts: The first is the setting up of matrices. This is done in parallel with the second part which is the calculation of error terms, i.e., the solution of the transfer equation with known source functions. The time required for these tasks scales linearly with n_ν, n_μ, n_τ, n_{tr} and tends to be negligible for large problems. The setting up of matrices in the range of optical depths from approximately $\tau_{\nu\mu} = 0.1$ to $\tau_{\nu\mu} = 10$ does not vectorize on current compilers. The solution of the transfer equation contains certain recursions which do not vectorize. Both times may be shortened by a reorganization of the program such that the innermost loop runs over frequency and angle instead over depth.

Of more importance is the third part of the program which is the calculation of the corrections in the population numbers. This is done by solving the grand matrix equation of dimension $n_{\text{dim}} = n_l \cdot n_\tau$. Fortunately this part vectorizes easily and the simple structure of the approximate matrix can be taken advantage of in a straightforward way without destroying the vectorization.

The grand matrix equation is solved as an ordinary two-dimensional matrix equation using *LU*-factorization. The absence of subdiagonal elements in the approximate matrix reduces the *number* of innermost do-loops without shortening the length of each of them, i.e., without reducing the advantage of vectorization. The absence of some of the elements above the diagonal reduces the length of innermost loops by typically a factor 2–4 without interfering with the vectorization. Thus the simple structure of the approximate matrix can be taken full advantage of also on a vectorizing machine such as the CRAY-1.

As one example we may take the time required to solve a five level + continuum calcium II problem with 109 depth points. Here the setting up of matrices, the calculation of error terms and the calculation of corrections took 1.41, 1.29, and 4.98 sec, respectively, for a total of five iterations. Suppressing vectorization increased these times to 2.15, 1.62, 22.86 sec showing that the most time-consuming part of the program vectorizes well. It should be added that the routine used for solving the matrix equation is not at all optimized for the CRAY and that considerably faster methods are available.

The program has also been used by Saxner [27] for solving the non-LTE problem for an F-star model atmosphere using 40 depth points and a model atom consisting of 17 levels + continuum. The total time required for a converged solution was only 18 sec.

To summarize, we think that the methods described in this paper are well suited also for vectorizing machines and that problems with say $n_\tau = 40$, $n_l = 35$ may be solved using not much more than a minute of computing time on a CRAY-1 having 3 M words of memory.

6. Concluding Remarks

We have described a new approach to the numerical solution of multi-level, non-LTE problems. The basic philosophy of this approach was to develop numerical methods from certain simplifications which are natural from analyzing the physics of the problem [5, 7]. It is the nonlocal components of the radiation field which

convinced that this approach to the solution of non-LTE problems will offer promising possibilities for future studies of complex problems involving radiative transfer, since it is much more efficient than other existing methods and also easier to generalize.

The multi-level method described in this paper is a complete linearization method which takes full account of the nonlocal and nonlinear interactions occurring in a radiating gas. The present method is simple: it involves no equivalent two-level iterations for initializing the solution, no lambda iterations for smoothing the solution and no SOR iterations to enhance the speed of solving the linearized rate equations, and it does not use the variable Eddington factors of Auer and Mihalas [24]. The present method is ideal for studies involving velocity fields and therefore has many important future applications. Finally, the method illuminates the physical nature of nonlocal radiative interactions in spectral lines and therefore should be of value for understanding the complicated thermodynamics occurring in a moving, radiating gas.

The present methods form the basis of a new general multi-level non-LTE

program [17]. Calculations made with this program have shown the methods to be stable, accurate, and very fast.

We have made some preliminary tests with a partial redistribution formulation similar to that of Scharmer [8]. The modifications were very easy to program, requiring only some 50 extra lines of coding. Tests made to solve Ca K problems indicate that the method works very well even though the convergence is somewhat slower than for the case of complete redistribution.

In addition we worked on a method for solving multi-dimensional problems which should be ideal for situations where vertical transfer effects are more important than horizontal transfer effects. It is based on the fact that the influence on the population numbers of the optically thin components of the radiation field can be corrected by lambda iteration and need not be taken explicitely into account when constructing the $\Lambda^\dagger$ operator. This implies that for situations where the horizontal length scale is much greater than the vertical length scale the matrices corresponding to horizontal transfer effects will be tridiagonal which considerably reduces both core storage requirements and the computing time required to solve the resulting very large matrix equations.

ACKNOWLEDGMENTS

One of the authors (G.S.) thanks the High Altitude Observatory (HAO) in Boulder and the Swedish Natural Science Research Council for a postdoctoral fellowship which made a 9-month stay at HAO possible. The same author is also grateful to Dr. D. Mihalas for his hospitality and for many stimulating conversations throughout the course of this work. Dr. Å. Nordlund is acknowledged for valuable discussions, especially concerning the use of diffusion corrections at large optical depths.

Mats Carlsson wants to thank the Institute of Theoretical Astrophysics in Oslo and the Nordic Council of Ministers for making the stay there possible. Dr. Kjell Eriksson and Dr. Bruce Lites are thanked for valuable discussions during the development of the program. Dr. Bengt Gustafsson, Dr. Wolfgang Kalkofen and Dr. Per Maltby are thanked for valuable comments on the manuscript.

REFERENCES

1. D. MIHALAS, "Stellar Atmospheres," 2nd ed., Freeman, San Francisco, 1978.
2. U. FRISCH AND H. FRISCH, *Mon. Not. R. Astron. Soc.* **173** (1975), 167.
3. R. C. CANFIELD, R. C. PUETTER, AND P. J. RICCHIAZZI, *Astrophys. J.* **248** (1981), 82.
4. G. B. RYBICKI, *in* "Methods in Radiative Transfer" (W. Kalkofen, Ed.), Cambridge Univ. Press, London, 1984, 21.
5. G. B. SCHARMER, *Astrophys. J.* **249** (1981), 720.
6. G. B. SCHARMER AND A. NORDLUND, Stockholm Observatory Report, Vol. 19, 1982.
7. G. B. SCHARMER, in "Methods in Radiative Transfer" (W. Kalkofen, Ed.), Cambridge Univ. Press, London, 1984, 173.
8. G. B. SCHARMER, *Astron. Astrophys.* **117** (1983), 83.
9. W. KALKOFEN, *Astrophys. J.* **188** (1974), 105.
10. G. B. RYBICKI, *in* "Line Formation in the Presence of Magnetic Fields" (R. G. Athay, L. L. House, and G. Newkirk, Jr., Eds.), p. 145 High Altitude Observatory, Boulder, Colo.

11. L. H. AUER AND D. MIHALAS, *Astrophys. J.* **158** (1969), 641.
12. G. B. RYBICKI, *J. Quant. Spectrosc. Radiat. Transfer* **11** (1971), 589.
13. G. B. RYBICKI AND D. HUMMER, *Mon. Not. R. Astron. Soc.* **144** (1969), 313.
14. W. KALKOFEN, *J. Quant. Spectrosc. Radiat. Transfer* **6** (1966), 633.
15. J. E. VERNAZZA, E. H. AVRETT, AND R. LOESER, *Astrophys. J. Suppl.* **45** (1981), 635.
16. B. LITES, Private communication, 1983.
17. M. CARLSSON, Uppsala Astronomical Observatory Report, **33**.
18. L. H. AUER AND J. N. HEASLY, *Astrophys. J.* **205** (1976), 165.
19. R. A SHINE AND J. L. LINSKY, *Sol. Phys.* **39** (1974), 49.
20. D. H. Sampson and L. B. Golden, *Astrophys. J.* **161** (1970), 321.
21. L. B. GOLDEN AND D. H. SAMPSON, *Astrophys. J.* **163** (1971), 405.
22. D. MIHALAS, *Astrophys. J.* **149** (1967), 169.
23. R. W. MILKEY AND D. MIHALAS, *Astrophys. J.* **185** (1973), 709.
24. L. H. AUER AND D. MIHALAS, *Mon. Not. R. Astron. Soc.* **149** (1970), 65.
25. L. H. AUER, *Astrophys. J.* **180** (1973), 469.
26. J. LEIBACHER, P. GOUTTEBROZE, AND R. F. STEIN, *Astrophys. J.* **258** (1982), 393.
27. M. SAXNER, *Astron. Astrophys.*, in press.